

# Modeling of de-NO<sub>x</sub> Reaction by Ammonia Radicals Generated from Atmospheric Plasma

Energy and Renewable Energy Systems Division, Graduate School of Engineering,  
Gifu University, Yanagido 1-1, Gifu, 501-1193  
Shinji Kambara, kambara@cc.gifu-u.ac.jp

## ABSTRACT

To reduce NO<sub>x</sub> emission from fossil fuel combustion, various experiments using plasma techniques have been studied. Different kinds of plasma reactors have been developed to remove NO<sub>x</sub> for high efficiency and low cost. However, energy efficiency (g-NO/kWh) is low in their techniques because large amount of exhaust gas are treated in plasma reactors with large power consumption. For improving energy efficiency, we have developed a new De-NO<sub>x</sub> system by direct ammonia radical injection. NO reduction experiment was performed by injecting ammonia radicals, which were externally generated by flowing the NH<sub>3</sub> gas diluted with Ar gas through a dielectric barrier discharge (DBD) with a one-cycle sinusoidal-wave power source. The generated radicals in the DBD were injected to simulation gas (NO/O<sub>2</sub>/N<sub>2</sub>). As a result, the maximum energy efficiency in this system was 140 g-NO/kWh.

In this report, we examined simulation models for chemical reaction in this experiment system to understand the reaction mechanisms in the reactor including DBD zone and reaction zone, and to improve de-NO<sub>x</sub> efficiency by using CHEMKIN.

## 1. INTRODUCTION

We have been developed the high efficiency NO reduction method by ammonia radical injection for using the radical chain reaction in a combustion process. There are some new technology using the radical reaction for NO reduction such as the plasma nozzle method and the electronic beam method. Fig.1-1 (a) and (b) show the outline figure of the plasma nozzle method and the electronic beam method. Unfortunately, these methods need a lot of power energy to excite all of flue gas with plasma or electronic beam. On the other hand, the radical injection method we propose, Fig.1-1 (c), is the method of exciting only a radical agent (NH<sub>3</sub>), the radicals are produced with little power. Therefore consumption power is lower than other methods and it is possible to reduce NO<sub>x</sub> on the cheap.

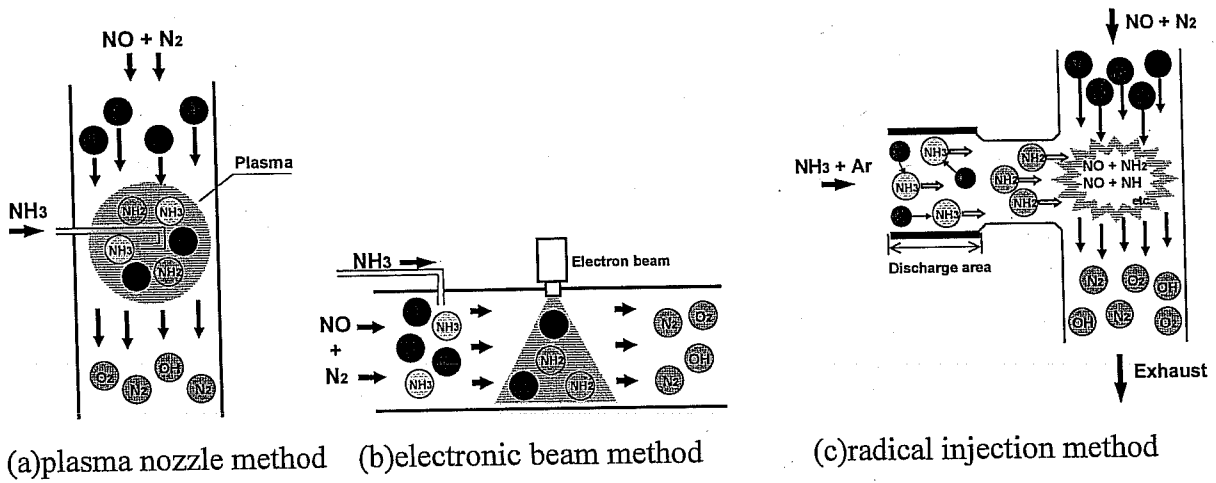


Fig.1-1 The existing NOx removal techniques using of plasma.

It is clear that the most effective radical of NO removal is  $\text{NH}_2$  radical from the traditional examination. Fig. 1-2 shows a key radical and a typical reaction of NOx reduction. In order to generate  $\text{NH}_2$  radicals from  $\text{NH}_3$  by plasma generated by DBD, it is clear that plasma must be generated with the small energy. In other words, when  $\text{N}_2$  gas with high voltage for generating plasma is used as career gas of a radical agent,  $\text{NH}_3$  is resolved into  $\text{NH}$  radicals or  $\text{N}$  radicals, and high efficiency NO reduction is not obtained. On the other hand, when  $\text{Ar}$  gas with low voltage for generating plasma is used as career gas of radical agent, it is presumed that a lot of  $\text{NH}_2$  radicals were produced, and high efficiency NO reduction is obtained.

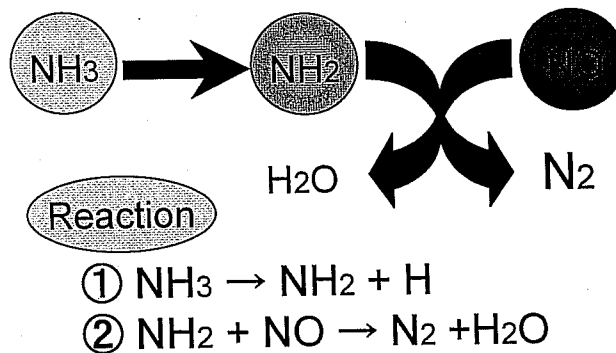


Fig. 1-2 The key radical and reaction of NO removal reaction.

## 2. EXPERIMENTAL AND CONDITIONS

Fig. 2-1 shows the experimental apparatus of radical injection method. The apparatus consists of three sections; radical injector, tube furnace with electric heater, and reaction chamber. Radical injector generates ammonia radicals ( $\text{NH}_i$ ) from the plasma generated by DBD. Tube furnace with electric heater heats simulated gas to a given temperature and it maintains mixed gas ( $\text{NH}_3 + \text{NO}$ ) of a given temperature, and a reaction is promoted. Reaction chamber makes

$\text{NH}_3$  and NO react. In detail, model gas ( $\text{NO}/\text{N}_2/\text{O}_2$ ) is pre-heated by tube furnace.  $\text{NH}_i$  radicals having rapid chemical reaction rate are externally generated by  $\text{NH}_3$  gas diluted with Ar gas through a DBD with a one-cycle sinusoidal-wave power source. NO concentration before and after plasma resolution is measured with the NOx meter installs in the exhaust gas side, and NO reduction is calculated. Therefore, NO reduction is defined by the equation (2-1).

$$\text{NO.reduction} = \frac{[\text{NO}]_i - [\text{NO}]_f}{[\text{NO}]_i} \times 100 \quad (2-1)$$

Applied voltage is varied 3 to 15 kV with repetition rate of 10 kHz. Reaction temperature is varied 341 to 483 °C.  $\text{NH}_3/\text{NO}$  mol fraction is varied 1.0 to 1.5.  $\text{O}_2$  concentration is varied 0 to 5 %. Residence time is varied 4.06 to 5.71 s.

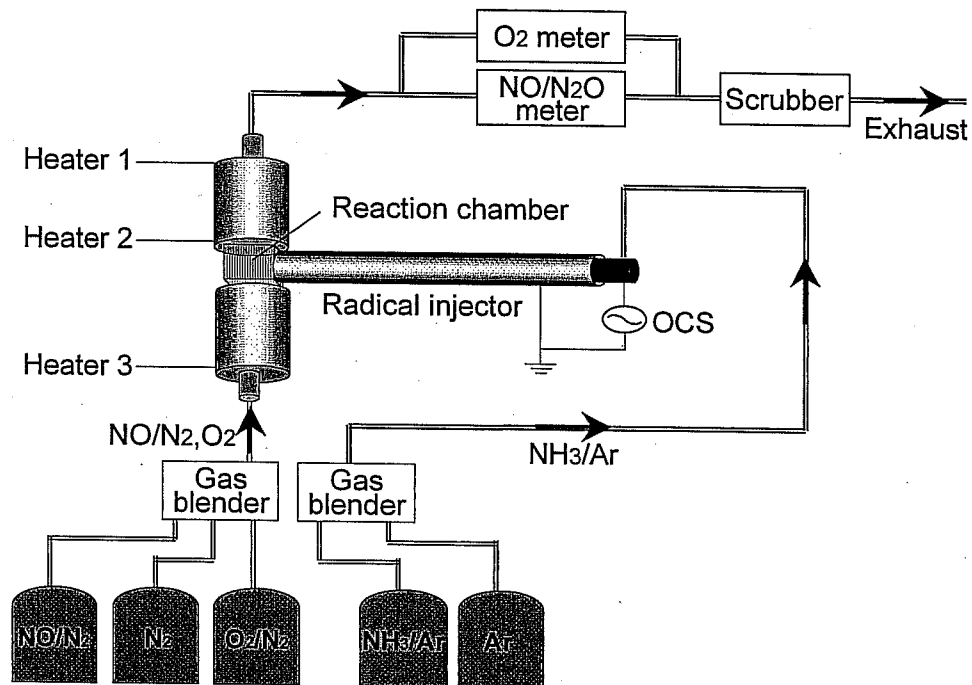


Fig. 2-1 Schematic diagrams of experimental apparatus.

### 3. RESULTS

Fig. 3-1 shows NO reduction at  $\text{O}_2$  concentration of 1% and  $\text{NH}_3/\text{NO}$  mole fraction of 1.5 and residence time of 5.71 s as a function of applied voltage. De-NOx occurs at applied voltage about 5 kV and NO reduction reaches 99.5% at 483 °C. However, NO reduction decreases when applied voltage is too high because plasma occurs by applied voltage and  $\text{NH}_3$  is decomposed into NH radicals or N radicals.  $\text{NH}_2$  radicals are more effective in NO reduction than NH or N radicals. Therefore, a lot of NH or N radicals are generated and NO reduction when the applied

voltage is too high.

Fig. 3-2 shows NO reduction at reaction temperature of 483°C and NH<sub>3</sub>/NO mole fraction of 1.5 and residence time of 5.71 s as a function of O<sub>2</sub> concentration. De-NO<sub>x</sub> occurs in the case of O<sub>2</sub> is included. In the case of applied voltage of 3 kV, it tends to increase the NO reduction with increasing O<sub>2</sub> concentration. On the other hand, in the case of 5 kV or more, it tends to decrease NO reduction with increasing O<sub>2</sub> concentration. From here onwards, O<sub>2</sub> generates OH that has an important role for the reduction reaction of NO. However, NH<sub>i</sub> radicals generated by applied voltage react with O radicals. In the result, NO reduction decreases when O<sub>2</sub> concentration is high because NO is re-generated.

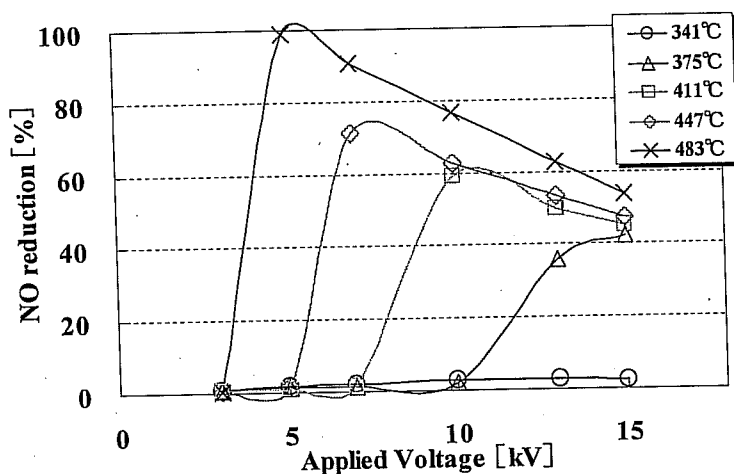


Fig. 3-1 NO reduction as a function of applied voltage.

(O<sub>2</sub> = 1%, NH<sub>3</sub>/NO = 1.5, residence time = 5.71 s, parameter = reaction temperature)

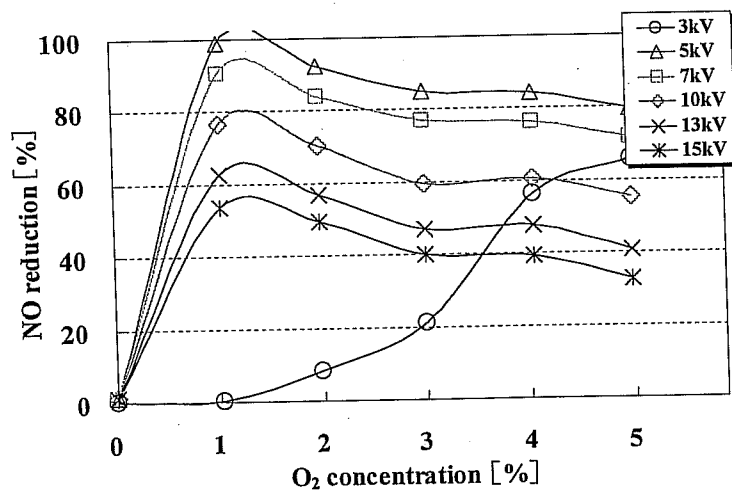


Fig. 3-2 NO reduction as a function of O<sub>2</sub> concentration.

(483°C, NH<sub>3</sub>/NO = 1.5, residence time = 5.71 s, parameter = applied voltage)

## 4. REACTION DYNAMICS CALCULATIONS

The above reaction dynamics calculations were performed with the SENKIN routine, which is an application in Reaction Design's CHEMKIN III software. SENKIN is a program that computes the time evolution of all species concentrations according to a detailed chemical reaction mechanism. For this application the calculations were performed for uniform temperatures and pressures throughout. Whereas these calculations are nominally zero-dimensional, they are exactly the same as those for one-dimensional, isothermal plug flows with no backmixing or radial dispersion, once the spatial coordinate has been converted into a residence time with a uniform velocity.

The NO reduction mechanism used for all calculations in this report was assembled by Glarborg and coworkers (Glarborg et al. 1998) for applications involving reburning and other interactions among nitrogen and hydrocarbon species. It is, by far, the most suitable mechanism in the combustion literature for this application because it is based on a laboratory database compiled with a flow reactor at temperatures from 525 to 1225 °C. The complete mechanism contains 444 elementary reactions, although we used an abridged set of 117 reactions involving only H/N/O species, because our current reaction system of interest contains no carbon.

### 4.1 Overview of the Testing System

The schematic diagram of the test facility appears in Fig. 4-1. It contains two flow channels, one vertical flowline for synthetic exhaust and one horizontal flowline for a flow with radicals. Flows into the radical injection line may contain NH<sub>3</sub> in either N<sub>2</sub> or Ar, N<sub>2</sub> in Ar, or pure N<sub>2</sub>. The radical injection line contains an annular channel that sustains dielectric barrier discharges along the region surrounding the electrode. This section is called the DBD zone. The discharges ionize and dissociate the deNO<sub>x</sub> agents, so that radicals, positive ions, and electrons are present at the end of the DBD zone. In addition, the radical injection line contains a connector region, from the end of the DBD to the right wall of the mixing chamber. The exhaust line begins with a heated section, called the preheat zone, that also connects into the mixing chamber. The mixing chamber is cubical, with two inlet flows, one circular and one annular, and one circular outlet flow. The mixed flows escape through the heated line at the top of the mixing chamber called the postheat zone.

All flow channels are made of quartz. The annular gap in the radical injector is 1.5 mm wide. The length of the DBD zone is 300 mm and the connector is 70 mm long. The connector temperature is assigned as the temperature of the mixing chamber. A linear temperature profile is assigned to the DBD zone, from the connector temperature to an inlet temperature of 250 °C.

The preheat zone is an electrically heated, 50 mm I. D. quartz tube in laminar flow. It is assumed to be isothermal. The postheat zone is identical and always operated at the same temperature as the preheat zone. However, the mixing chamber is always considerably cooler than the preheat and postheat zones.

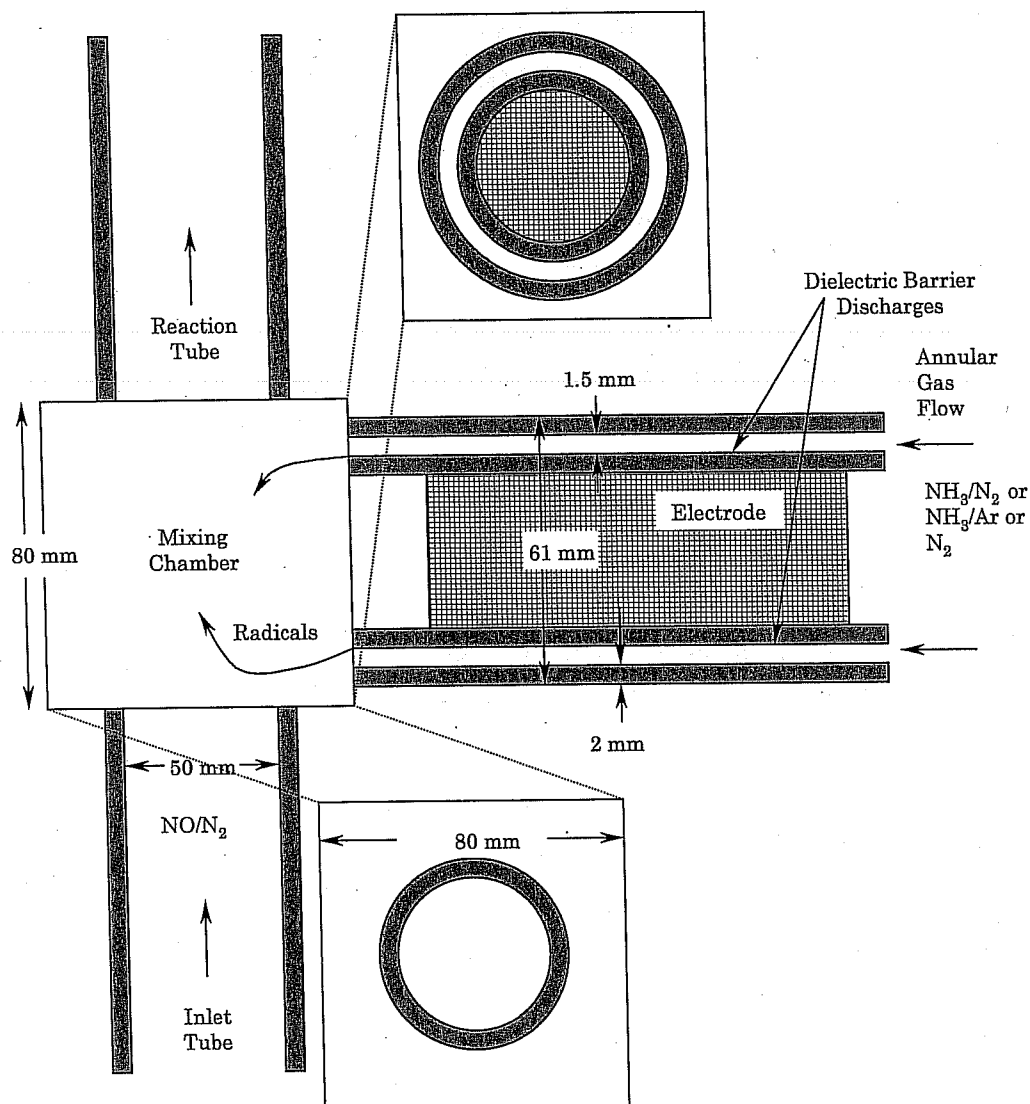


Figure 4-1. Schematic of the direct radical injection test facility.

Whereas the flow configuration in the test facility is relatively simple, this apparatus supports five separate regions, each with its own distinctive chemical and transport aspects. The mechanistic regions are illustrated in Fig. 4-2. The following five different chemical reaction mechanisms were used to classify these regions:

- (1) Radiolysis – Production of radicals, electrons, and positive ions within the localized plasma zones in the DBD zone only.
- (2) Charge Transfer – reactions in which primary positive ions react with stable species and radicals to form new positive ions.
- (3) Neutralization – reactions in which positive ions recombine with electrons to form stable species and radicals.
- (4) Recombination – reactions in which radicals combine to form stable species.
- (5) NO Conversion – radical chain reaction mechanism for reduction of NO.

Radiolysis only occurs in the DBD zone. In fact, in dielectric barrier discharges like this test

facility, radiolysis is confined to extremely fine, cylindrical plasmas that shoot across the gap in the DBD, like miniature lightning bolts. The plasma structures are called "streamers" in this context. Whereas radiolysis is confined to the streamers, it is not the only chemistry in the DBD zone. In the bulk gases moving through the DBD, primary radicals, ions, and electrons react continuously. These subsequent reactions are classified as charge transfer mechanisms, which conserve the number of positive ions, neutralization mechanisms, which restore charge neutrality, and recombination mechanisms, which eliminate radicals. Hence, four chemical mechanisms determine the behavior in the DBD zone.

The connector zone has no plasma; consequently, it cannot sustain radiolysis. But charge transfer, neutralization, and recombination in the connector will significantly affect the radical concentrations that actually enter the mixing chamber.

There are no sources of radicals in the preheater other than the thermal decomposition of NO, which is negligible at even the highest temperatures imposed in the testing program. Whereas NO reduction in the postheater is also negligible, the mixing chamber sustains radical chain reaction chemistry that significantly alters the NO concentration under almost all test conditions.

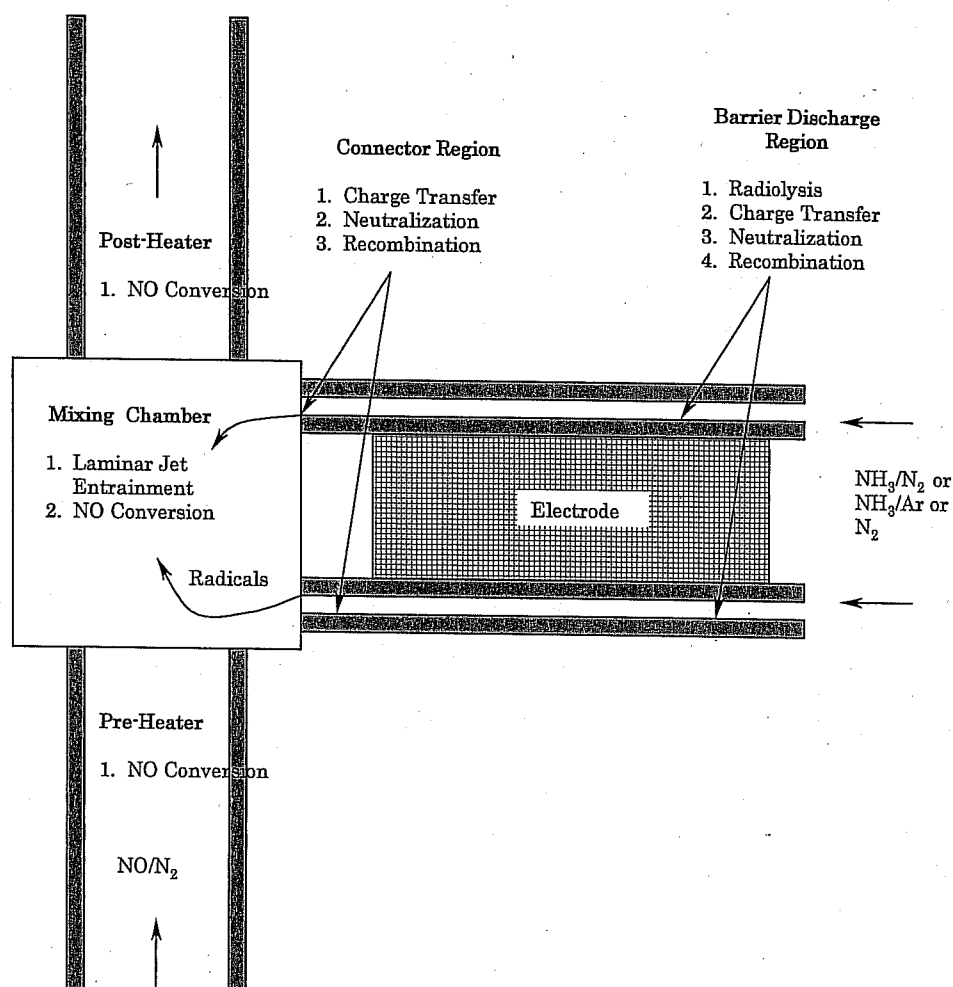


Figure 4-2. Five mechanistic regions in the direct radical injection test facility.

## 4.2 Process Simulation Software

The submodels for the five mechanistic regions in the test apparatus were combined into an overall process simulator that accepts input data, sequences through all stages of the calculations, then prepares the output report forms. The ODEs associated with the mechanisms in the DBD and connector zones were solved with library subroutines, while those for the pre- and post-heaters and the mixing chamber were solved with CHEMKIN. Perhaps the most important feature of CHEMKIN for this application is that it is very easy to execute repeated calls to any of the programs in CHEMKIN by an external, user-defined program written in C++ or FORTRAN.

The required input data are collected in Table 4-1. They consist of sufficient geometrical information to assign nominal flow velocities, component temperatures and the system pressure, the inlet flowrates and compositions into the radical injector arm and exhaust line, and the voltage and repetition rate used to charge the DBD electrode.

## 4.3 Process Simulation Results

In this section, we show process simulation results by CHEMKIN for NO reduction with  $\text{NH}_3$  radicals under  $\text{N}_2$  plasma.

According to the reaction mechanism proposed for injection of  $\text{NH}_3$  in  $\text{N}_2$  into the DBD zone, the abundance of N-atoms (from radiolysis of  $\text{N}_2$ ) near-instantaneously disintegrates the  $\text{NH}_3$  into additional N-atoms. The associated H-atoms very rapidly recombine to form  $\text{H}_2$ . Hence, the performance of the DBD zone in this case is predicted to be very similar to the pure  $\text{N}_2$  case, except for slightly higher N-atom concentrations and for the presence of small amounts of  $\text{H}_2$ . Consequently, we also expect similar NO reduction efficiencies.

The dataset in Fig. 4-3 verifies this interpretation. For the same discharge voltage and rep rate, the NO reduction efficiencies for  $\text{NH}_3$  injection are slightly higher than those for pure  $\text{N}_2$ . Generally speaking, the predictions for  $\text{NH}_3$  are also slightly more accurate.

The predictions are within experimental uncertainty for 45 and 40 kV across the entire range of rep rate. But for voltages below 35 kV the predictions are higher than the observed NO reduction efficiencies, especially as the lower rep rates. With 25 kV, the predictions are almost 10 % higher than the measured values across the entire range of rep rate.

Extremely accurate predictions are also apparent in the evaluation of the onset of NO reduction with  $\text{NH}_3$  injection in Fig. 4-7. The data show that no NO reduction occurs below 22 kV, then the reduction efficiency increases in direct proportion to increases in the discharge voltage. Unlike the pure  $\text{N}_2$  case, there is no saturation level with  $\text{NH}_3$ . The predictions also show no NO reduction below a threshold voltage, but the predicted threshold value is only about 14 kV. Then the predicted efficiencies increase sharply at first, then in direct proportion to the discharge voltage thereafter. No saturation level is evident in the prediction NO reduction efficiencies, and the predicted values are within experimental uncertainty for voltages above 33 kV.



Table 4-1. Required Input Parameters

Parameter, Units	Definition
<b>DBD Zone</b>	
$T_0$ , °C	Inlet temperature
$T_{DBD}$ , °C	DBD outlet temperature
P, atm	System operating pressure
$L_{DBD}$ , cm	Length of the electrode in the DBD
$D_{DBD}$ , cm	Inside diameter of the DBD flow channel
S, cm	Height of the DBD flow channel
$Q_{DBD}$ , slpm	Gas flowrate in DBD zone
$x_i$	Mole fractions of N <sub>2</sub> , NH <sub>3</sub> , and Ar
$G_i$	G-Factors for all radiolysis species
$V_{pp}$ , kV	Peak-to-peak voltage
RR, kHz	Pulse repetition rate
<b>Connector Zone</b>	
$T_{CON}$ , °C	Connector zone temperature
$L_{CON}$ , cm	Connector length
<b>Preheater Zone</b>	
$T_{PRE}$ , °C	Preheater temperature
$L_{PRE}$ , cm	Preheater length
$D_{PRE}$ , cm	Diameter of the preheater flow channel
$Q_{PRE}$ , slpm	Gas flowrate into the preheater
$x_i$	Mole fractions of NO and N <sub>2</sub>
<b>Mixing Chamber</b>	
$T_{MIX}$ , °C	Mixing chamber temperature
$L_{MIX}$ , cm	Wall length
<b>Postheater Zone</b>	
$T_{PST}$ , °C	Postheater temperature
$L_{PST}$ , cm	Postheater length
$D_{PST}$ , cm	Diameter of the preheater flow channel

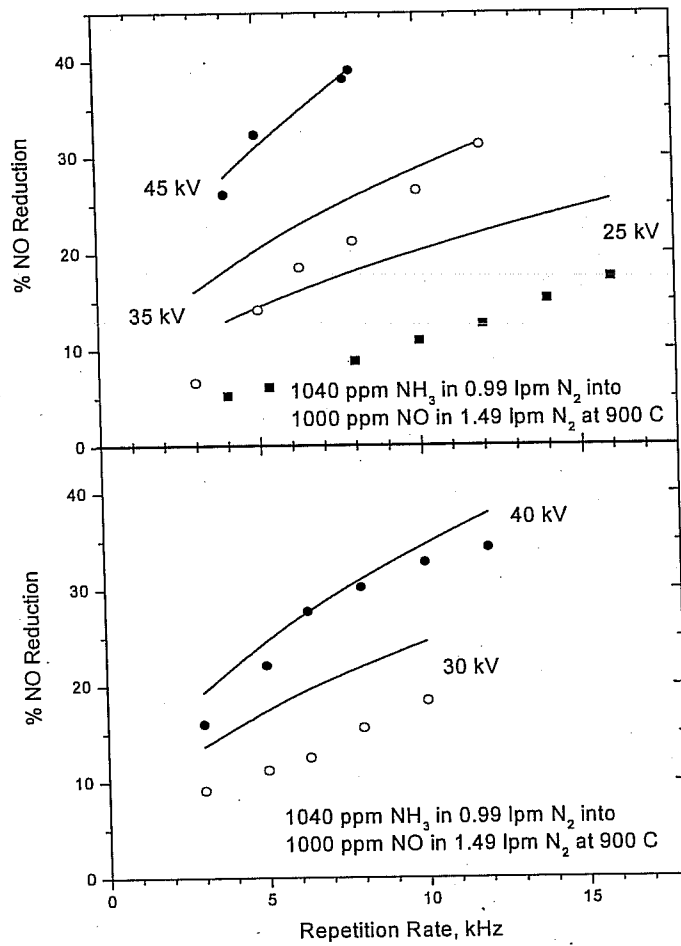


Figure 4-6. Evaluation of predicted NO reduction efficiencies by NH<sub>3</sub> versus repetition rate for discharge power levels of (Top) 25, 35, and 45 kV and of (Bottom) 30 and 40 kV.

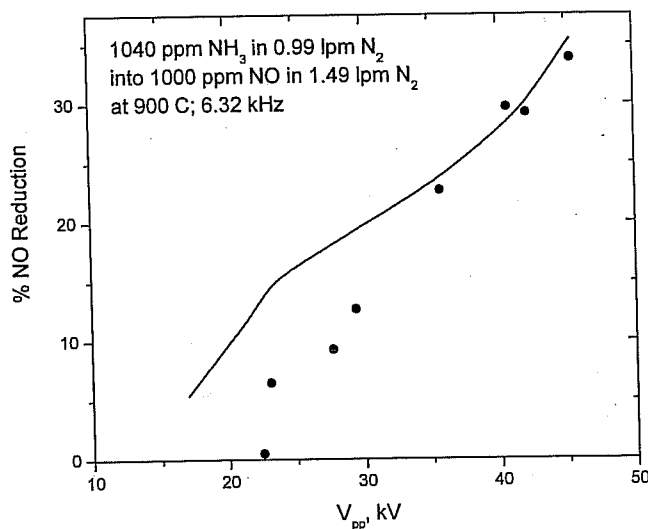


Figure 4-7. Evaluation of predicted onset of NO reduction by NH<sub>3</sub> over a range of discharge

voltages.

## CONCLUSION

The submodel for the DBD zone describes radiolysis, charge transfer, neutralization, and recombination chemistry in terms of elementary reaction mechanisms. Rates of electron impact in streamers were based on a Maxwell-Boltzmann energy distribution with step function cross sections. Drift velocities and the transport and reaction rates were based on the assigned electron energy distribution function. Ultimately, the reaction rates and distributions of positive ions, radicals, and electrons were expressed as a global process that explicitly depends on the discharge power, hence, on the voltage and repetition rates in the discharge.

The submodel for the connector into the mixing chamber simply reduced the concentrations of activated species by a fixed percentage. Eighty percent reduction was applied to all cases, and no adjustments were made to fit predictions to data.

An elementary reaction mechanism with 117 steps was used to model NO reduction in the pre- and post-heaters. No chemistry was predicted to occur in these sections at even the highest operating temperatures because the thermal decomposition of NO was the only source of radicals. The mixing chamber was modeled with the same detailed mechanism for NO conversion in two CSTRs in series that represented the backmixing and entrainment patterns in the actual device. The first CSTR was fed by the entire exhaust flow plus half the flow from the radical injector. The second CSTR was fed by the exhaust from the first plus the other half of the flow from the radical injector.

Predicted NO reduction efficiencies were within experimental uncertainty at the highest discharge voltages. But the predictions overestimated the performance at lower voltages, usually by up to ten percentage points in NO reduction efficiency. The simulator also depicted the main features of the onset of NO reduction. No NO reduction occurred below a threshold voltage, then the reduction efficiency increased rapidly for higher voltages. But the predicted threshold voltage was too low for NH<sub>3</sub> in N<sub>2</sub>.

## ACKNOWLEDGEMENTS

The author wish to thank Dr. S.Niksa, predident of NEA corporation, USA, for his help in the valuable suggestions in this study.

